Inverse silica opal photonic crystals for optical sensing applications

Y. Nishijima[1], K. Ueno[1], S. Juodkazis[1], V. Mizeikis[1], H. Misawa[1*], T. Tanimura[2], and K. Maeda[2]

[1] *Research Institute for Electronic Science (RIES), Hokkaido University, CRIS Bldg., Kita 21 Nishi 10, Kita-ku Sapporo 001-0021, Japan*
[2] *Sanyo Chemical Industries, Ltd., Ikkyounomotocho 11-1, Higasiyama-ku Kyoto 605-0995, Japan*
[*] *corresponding author e-mail: misawa@es.hokudai.ac.jp.*

Abstract: This work reports fabrication of inverse silica opal photonic crystal structures from direct polystyrene micro sphere opals using low-temperature sol-gel infiltration of silica, and examines performance of these photonic crystals as environmental refractive index sensors. Sensitivity of the spectral position and optical attenuation of photonic stop gaps is found to allow detection of the index changes by the amount of ~10^{-3}. The high value of sensitivity, which is comparable with those of other optical sensing techniques, along with simplicity of the optical detection setup required for sensing, and the low-temperature, energy-efficient fabrication process make inverse silica opals attractive systems for optical sensing applications.

OCIS codes: (230.5298) Photonic crystals; (350.4238) Nanophotonics and photonic crystals

References and links

1. S. John, "Strong localization of photons in certain disordered dielectric superlattices," Phys. Rev. Lett. **58**, 2486–2489 (1987).
2. E. Yablonovitch, "Inhibited spontaneous emission in Solid-State Physics and Electronics," Phys. Rev. Lett. **58**, 2059–2062 (1987).
3. A. Blanco, E. Chomski, S. Grabtchak, M. Ibisate, S. Jhon, S. W. Leonard, C. Lopez, F. Meseguer, H. Miguez, J. P. Mondia, G. A. Ozin, O. Toader and H. M. van Driel, "Large-scale synthesis of a silicon photonic crystal with a complete three-dimensional bandgap near 1.5 micrometres," Nature **405**, 437-440 (2000)
4. H. Fudouzi and Y. Xia, "Photonic papers and inks: color writing with colorless materials," Adv. Mater. **15**, 892–896 (2003).
5. J. H. Holtz and S. A. Asher, "Polymerized colloidal crystal hydrogel films as intelligent chemical sensing materials," Nature **389**, 829 (2003).
6. H. Altug and J. Vučkovič, "Polarization control and optical sensing with two-dimensional coupled photonic crystal microcavity arrays," Opt. Lett. **30**, 982–984 (2005).
7. E. Chow, L. Mirkarimi, M. Sigalas, and G. Girolami, "Ultracompact biochemical sensor built with two-dimensional photonic crystal microcavity," Opt. Lett. **29**, 1093–1095 (2004).
8. T. Prasad, D. M. Mittleman, and V. L. Colvin, "A photonic crystal sensor based on the superprism effect," Opt. Mater. **29**, 5659 (2006).
9. M. C. Phan Huy, G. Laffort, Y. Frignac, V. Dewynter-Marty, P. Ferdinand, P. Roy, J-M. Blondy, D. Pagnoux, W. Blanc and B. Dussardier " Fibre Bragg grating photowriting in microstructured optical fibres for refractive index measurement." Meas. Sci. Technol. **17**, 992-997 (2006).
10. T. Ritari, J. Tuominen, H. Ludvigsen, J. Petersen, T. Sørensen, T. Hansen, and H. Simonsen, "Gas sensing using air-guiding photonic bandgap fibers," Opt. Express **12**, 4080–4087 (2004).
11. A. Baryshev, R. Fujikawa, A. Khanikaev, A. Granovsky, K. Shin, P. Lim, and M. Inoue, "Mesoporous photonic crystals for sensor applications," in *Proceedings of the SPIE, Photonic Crystals and Photonic Crystal Fibers for Sensing Applications II*. H. H. Du, R. Bise, eds., (2006), *pp.* 63690B.
12. S. Matsuo, T. Fujine, K. Fukuda, S. Juodkazis, and H. Misawa, "Formation of free-standing micro-pyramid colloidal crystals grown on silicon substrate," Appl. Phys. Lett. **82**, 4283–4285 (2003).
13. V. Mizeikis, S. Juodkazis, A. Marcinkevicius, S. Matsuo, and H. Misawa, "Tailoring and Characterization of Photonic Crystals," J. Photochem. Photobiol. C **2**, 35–69 (2001).
14. S. Juodkazis, E. Bernstein, J.-C. Plenet, C. Bovier, J. D. J. Mugnier, and J. V. Vaitkus, "Waveguiding properties of CdS-doped $(Si_{0.2}Ti_{0.8})O_2$ films prepared by sol-gel method," Thin Solid Films **322**, 238–244 (1998).

#86262 - $15.00 USD Received 9 Aug 2007; revised 18 Sep 2007; accepted 18 Sep 2007; published 25 Sep 2007

15. S. Juodkazis, E. Bernstein, J.-C. Plenet, C. Bovier, J. D. J. Mugnier, and J. V. Vaitkus, "Optical Properties of CdS Nanocrystallites Embedded in $(Si_{0.2}Ti_{0.8})O_2$ Sol-Gel Waveguide," Opt. Commun. **148**, 242–248 (1998).
16. R. C. Schroden, M. Al-Daous, C. F. Blanford, and A. Stein, "Optical properties of inverse opal photonic crystals," Chem. Mat. **14**, 3305–3315 (2002).
17. D. L.Wood, E. M. Rabinovich, J. D.W. Johnson, J. B. MacChesney, and E. M. Vogel, "Preparation of high-silica glasses from colloidal gels: III Infrared spectrophotometric studies," J. Am. Ceram. Soc. **66**, 693 – 699 (1983).
18. S. Sakka and J. D. Mackenzie, "Relation between apparent glass transition temperature and liquids temperature for inorganic glasses," J. Non-Cryst. Solids **6**, 145 – 162 (1971).
19. Y. Nishijima, *et al*., to be published (2007).
20. J. D. Joannopoulos, R. D. Meade, and J. N. Winn, *Photonic Crystals: Molding the Flow of Light* (Princeton University Press, Princeton, New Jersey, 1995).
21. J. Ye, R. Zentel, S. Arpiainen, J. Ahopelto, F. Jonsson, S. G. Romanov, and C. M. S. Torres, "Integration of self assembled three-dimensional photonic crystals onto structured silicon wafers," Langmuir 22, 7378–7383 (2006). URL http://dx.doi.org/10.1021/la0607611.
22. K. Yoshino, S. Satoh, T. Shimoda, H. Kajii, T. Tamura, Y. Kawagishi, T. Matsui, R. Hidayat, A. Fujii, and M. Ozaki "Tunable optical properties of conducting polymers infiltrated in synthetic opal as photonic crystal" Synthetic Met. **121**, 1459-1462 (2001).

1. Introduction

Photonic crystals (PhC) [1-3] are promising materials for applications in optoelectronics and photonics as well as in the field of optical sensing. Photonic crystal sensors exploit sensitivity of PhC dispersion bands to the modification of their refractive index and periodicity modulation by gases or fluids [4, 5]. PhCs are dielectric or metalodielectric materials whose periodic spatial variation of dielectric function is achieved using advanced micro- and nano-structuring techniques and leads to formation of spectral photonic band gaps (PBG) or stop gaps (PSG). Within these intervals propagation of electromagnetic waves is forbidden along all (for PBG) or along specific directions (for PSG). Most PhCs consist of permeable dielectric (or metalodielectric) networks open to gaseous or fluidic flows. Optical sensing can be realized in the simplest form by detecting modification of the PBG or PSG spectral signatures in the PhC reflectivity or transmission spectra due to the infiltration of PhC voids by various materials. More sophisticated sensing techniques exploiting resonant PhC microcavity states [6, 7], superprism effects [8], and optical interactions in photonic crystal fibers [9, 10] have been recently also developed.

Although three-dimensional (3D) PhC structures are not required for the optical sensing, which is possible with simpler one-dimensional (1D) or two-dimensional (2D) PhCs, artificial 3D opal PhC structures can be attractive as optical sensors [11]. First, their fabrication from colloidal suspensions of commercially available silica or polystyrene microspheres was perfected during the recent decades [12, 13]. Second, optical sensing is perhaps the only field of application for as-fabricated opal structures, which have no PBG due to the low index contrast between the closely-packed silica (n = 1.47) or polystyrene (n = 1.57) spheres and surrounding air (n = 1.0). Nevertheless they still retain one or several PSGs that can be utilized for optical sensing. Third, existence of multiple PSG regions along different directions in the 3D opal might add an interesting capability of performing simultaneous optical sensing at several wavelengths along different directions.

This work addresses the fabrication and application of silica inverse opal structures as simple optical fluidic sensors. Although use of various direct and inverse opal photonic crystals for optical sensing has been addressed before, suitability of inverse silica opals for this purpose has not yet been examined. The results of the present study clearly demonstrate that sensors based on silica inverse opals have several important advantages compared to other opal-based or photonic crystal-based sensors. Below we will briefly outline these advantages. First of them is that opal inversion is performed by infiltrating the initial direct template composed of polystyrene microspheres, with silica glass using a low-temperature sol-gel process, and by subsequently removing the template. The low-temperature silica infiltration is an energy-efficient process, which nevertheless produces high-quality periodic

#86262 - $15.00 USD Received 9 Aug 2007; revised 18 Sep 2007; accepted 18 Sep 2007; published 25 Sep 2007

networks of silica. High thermal and chemical stability of silica glass allows performance of optical sensing in a wide temperature range in a variety of fluidic environments. The next potential advantage stems from general properties of inverse opals. The inverse silica opal consists of closely packed spherical air voids arranged in a face-centered cubic (fcc) point lattice, and embedded in a framework of solid silica. Since inverse silica opal would have the same or even lower index contrast than the initial polystyrene template, use of inverted opals at a first glance promises no significant improvement. To clarify this issue it is helpful to consider analytical expression for the spectral position of the fundamental (lowest frequency) PSG of 3D opal structures. For example, along the direction perpendicular to the (111) crystal planes, the PSG central wavelength λ_c can be deduced from Bragg condition:

$$\lambda_c = 2d\sqrt{\frac{2}{3}[\, f_{sph}\, n_{sph}^2 + (1 - f_{sph})\, n_{bg}^2\,]} \qquad (1)$$

Where d is diameter of the spheres, f_{sph} is the sphere volume filling fraction, n_{sph} is the refractive index of spheres, and n_{bg} is the "background" refractive index of the empty regions, or voids between the spheres. Closely packed opals have sphere filling fraction $f_{sph} = 0.74$, while the voids fill the remaining $1 - f_{sph} = 0.26$ fraction of the volume. In direct opal n_{bg} can be altered by the infiltration of other materials into the voids, whereas n_{sph} is the constant refractive index of spheres. In inverse opal n_{sph} represents voids whose refractive index can be altered by infiltration, whereas n_{bg} is the constant refractive index of solid dielectric framework. According to Eq. (1) the PBG wavelength is more sensitive to the variations of n_{sph} than of n_{bg} due to the larger sphere volume-filling fraction. Although this circumstance is quite obvious, so far it has not been exploited for improving accuracy of opal PhC sensors. The refractive index sensing limit obtainable with PhCs fabricated and investigated in this work is estimated to be about 10^{-3}. This value is quite high and can be regarded as another potential advantage of inverse silica opal structures, since it is close to that reported for two-dimensional PhC microcavities [7] prepared using advanced semiconductor nanofabrication techniques. Recently, a novel optical sensing scheme using opal PhC and based on superprism effect was reported to provide sensitivity of 10^{-5} [8]. Although performance of such sensor is superior to ours, it also requires a more complex optical setup. Sensitivity of about 10^{-3}, i.e., similar to ours, was also reported recently for optically-structured photonic crystal fibers [9] (It is difficult to compare sensitivity of our opal structures with that of some other 2D photonic crystal fibers [10], since they are used for gas sensing exploiting absorption of the optical radiation, rather than its refraction).

Here we report fabrication of synthetic opal PhC structures from polystyrene microspheres having various diameters, and subsequent inversion of these templates with silica glass using low-temperature sol-gel process and removal of the template. By comparing optical properties of the direct and inverse opal structures we demonstrate that in accordance to the expectations, inverse silica opals exhibit higher environmental sensitivity. These findings may help improve optical sensors based on opal PhC structures.

2. Experimental details

Preparation of the initial polystyrene templates was done by centrifuged sedimentation (6900, KUBOTA, Co.) of polystyrene spheres (Sekisui, Inc.) at 5000 rpm (4200 G) for 10 min on cover glass substrates. The centrifuged sedimentation process is shown schematically and explained in Fig. 1. Spheres with different diameters of d = 220, 320, 400, 520, and 600 nm were used. After the centrifugation the structures were dried and annealed at 90ºC for 3 min. Figure 2(a) shows Scanning Electron Microscope (SEM) image of as-fabricated direct opal structure. The sol-gel formation of inverse silica opal structure was performed by immersion of the samples into a tetraethoxysilane sol, and subsequent drying at 90ºC for 1 hour.

#86262 - $15.00 USD Received 9 Aug 2007; revised 18 Sep 2007; accepted 18 Sep 2007; published 25 Sep 2007

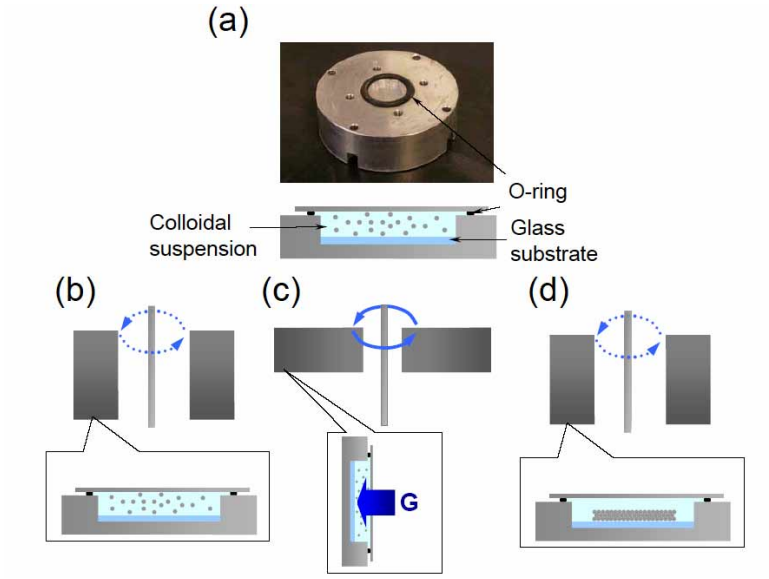

Fig. 1. Schematic explanation of centrifuged sedimentation process. Glass substrates are mounted in cylindrical pits of the sample holders containing about 0.2 ml of colloidal microspheres suspension, and sealed at the top by glass slides (a), the sample holders are placed at the bottom of larger hollow cylindrical holders (indicated by black rectangles), which are attached to the axle of the centrifuge by swivel-mounts, and are oriented vertically by the gravity force when the centrifuge is at standstill (b), when the centrifuge is turned on, centrifugal forces overcome the gravity, aligning the holders horizontally, and govern sedimentation from the colloidal suspension in the sample holders (c), after the centrifugation the cylindrical holders realign vertically, a film of synthetic opal having uniform thickness is obtained on the glass substrate (d).

The polystyrene template was then removed by immersion in ethyl acetate. No further high temperature sintering of gel was employed. The resulting inverse opal structure is shown in Fig. 2(b). The SEM images allow clear identification of the (111) fcc lattice plane.

Optical reflection spectra of the samples were measured using micro-spectroscopic setup consisting of an optical microscope (BX-51, Olympus Co.) equipped with an objective lens with x40 magnification and numerical aperture of NA = 0.75, using halogen lamp (Usio, Inc.) broadband illumination, and a multi-channel photodetector (PMA-11, Hamamatsu Photonics, Inc.). Infrared (IR) reflection spectra were measured using a Fourier-Transform Infrared (FTIR) spectrometer equipped with an IR microscope attachment (FT-IR, IRT-3000, Jasco, Inc.), employing a Cassegrainian objective lens with maximum NA = 0.5. With both measurement setups the samples were oriented with (111) crystallographic planes normal to the optical axis. In reciprocal space this orientation corresponds to the Γ-*L* direction. To mimic the environments of different refractive index, samples were immersed into a range of organic solutions: fluorinert FC72 (n = 1.24), fluorinert FC77 (n = 1.26), methanol (n = 1.33), ethanol (n = 1.36), 2-propanol (n = 1.37), and propylene carbonate (n = 1.42).

3. Results and discussion

3.1. Structural properties of PhC structures and uniform silica glass obtained via sol-gel route

Good periodic ordering of the direct and inverse opal PhCs prepared for this work were already illustrated by SEM images in Fig. 2. In addition to periodic opal structures, we have briefly studied properties of uniform silica films prepared via the same low-temperature sol-gel route as used for the opal inversion.

#86262 - $15.00 USD Received 9 Aug 2007; revised 18 Sep 2007; accepted 18 Sep 2007; published 25 Sep 2007

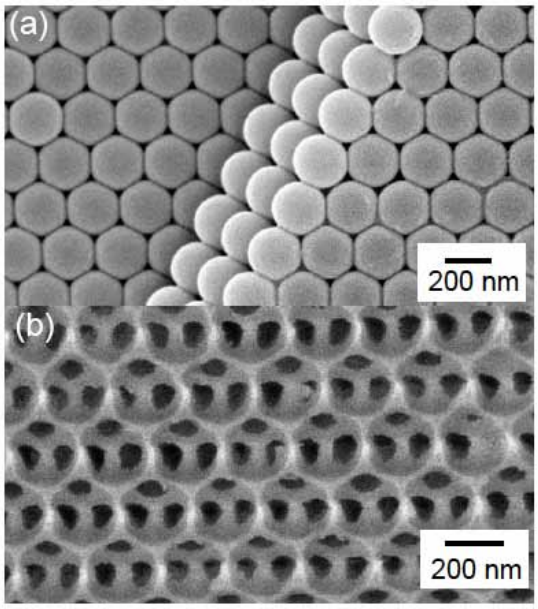

Fig. 2. SEM images of (111) surface of polystyrene direct opal PhC structure with sphere diameter of 220 nm (a), and of a similar structure after its inversion by silica (b).

Films with thickness of about 100 μm exhibit transmission T = 0.8 (limited mostly by Rayleigh scattering) in the wavelength range from 350 to 1700 nm. This proves the possibility to obtain films of high optical quality by energy-efficient method, which does not require high-temperature annealing of gel (annealing at high temperature is usually required in order to sinter gel for obtaining optical quality uniform silica-titania films [14, 15] and inverted opals in zirconia [16]). Additional treatment at elevated temperature can improve optical quality of glass even further: annealing at 520ºC for 2 hr resulted in considerable reduction of Rayleigh scattering in the 200-400 nm wavelength range and an increase of transmission to T > 90% in the wavelength range from 250 nm to 1.7 μm. The network of water vibrational bands hydrogen-bound to SiOH near the 1.4 and 1.9 μm wavelengths become weakened by sintering resulting from the annealing [17]. It is noteworthy that the highly-transmissive silica was obtained using gel processing temperatures three times lower than the glass transition temperature, T_g. Glasses usually need annealing at T_g for the release of stress and removal of defects ($T_g = 2T_m/3$, where T_m is the melting temperature. For silica T_m = 1723°C [18]). Hence, sol-gel synthesis performed in this work can be categorized as a low-temperature process (even if elevated temperatures were used) and may help provide silica glass for demanding optical applications, such as inverted opal PhC structures. It must be noted that high optical damage threshold of silica makes silica-inverted opals suitable for applications that require optical pumping (such as lasing of dyes infiltrated into opal PhC). For example, zirconia and titania inverted opals can be easily damaged at fluences above 0.1 GW/cm^2, whereas silica structures survive under the same conditions [19].

3.2. Optical properties of direct and inverse opals

Figure 3 summarizes the optical properties of direct and inverse opal structures in air. Detailed examination of optical reflectivities of the samples has revealed presence of a single major reflectivity peak in each of them. The measured peak wavelengths are close (albeit not exactly coincident) to the central wavelengths of the fundamental PSG inferred from Eq. (1). The relative mismatch between the experimentally measured and calculated values of λ_c was about 1% for direct and 4-7% for inverse structures; in the latter case shrinkage of silica sol during drying and the corresponding reduction of opal lattice period is the most likely origin

#86262 - $15.00 USD Received 9 Aug 2007; revised 18 Sep 2007; accepted 18 Sep 2007; published 25 Sep 2007

of mismatch. As can be seen from Fig. 3, in both kinds of samples the peak central wavelength λ_c scales nearly linearly with the sphere diameter or PhC lattice period. Such scaling is a characteristic feature of PBG and PSG materials, known as Maxwell's scaling property [19]. By varying the sphere diameter, the PSG wavelength can be tuned across the visible and near-infrared (NIR) spectral ranges. Since in inverse opal structures only 26% of volume is high-index material and the rest is air, their average refractive index is somewhat lower than that of direct polystyrene templates. Consequently, their PSGs are somewhat blue-shifted, which is another manifestation of the Maxwell's scaling. For the spheres of smallest diameter, d = 220 nm, the PSG of inverse opal structure is tuned beyond the shortest observation wavelength of 530 nm and therefore is absent in Fig. 3(b).

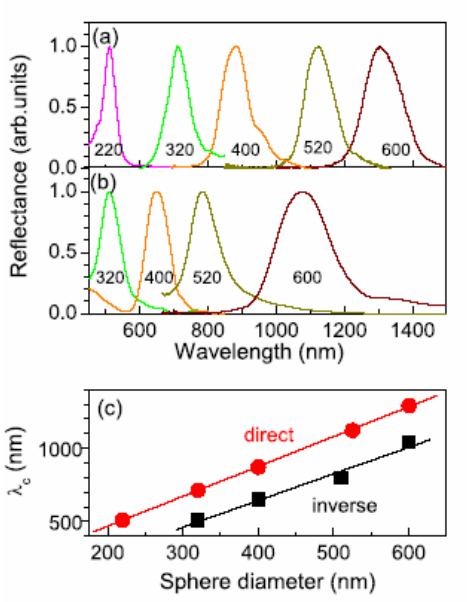

Fig. 3. Optical and IR reflectivities of direct of polystyrene opal (a) and inverse silica opal (b) PhC structures in air, and summary of the dependence of the peak wavelength λ_c on the sphere diameter (c) for opal and inverse opal structures. Total thickness of the structures is 100 μm. Relative statistical variations of λ_c values are less than 1%.

Next, we turn our attention to spectral variations in the reflectivities of opal structures due to infiltration of voids by different solutions. Figure 4 gives comparison between the reflectivities of direct and inverse opals with the same sphere diameter (d = 520 nm) in air and in various liquid solutions. Both samples exhibit red shift of the wavelength λ_c with refractive index. However, this trend is noticeably more pronounced for the inverse opal, as can be seen by comparing the spectra for n = 1.24 and 1.26 in both samples. It will be examined in more detail later (see Fig. 7 and the accompanying discussion). Spectral shifts deduced from Fig. 4, and also from spectra of other samples with different sphere diameters, are summarized in Fig. 5. The figure clearly illustrates linearity of the λ_c (n) dependencies. Inverse opal samples exhibit somewhat steeper slopes than the direct opals, in qualitative agreement with Eq. (1). However, the above equation cannot provide quantitative fits to the experimental data. Although this circumstance is not really a disadvantage for sensing applications, which would rely on empirical calibration of the λ_c (n) dependency (and its linearity) rather than on theoretical predictions, it is helpful to point out the most likely reason for the discrepancy between Eq. (1) and the experiments. Reflectivity measurements along the (111) direction should ideally use a collimated parallel beam propagating along that direction.

#86262 - $15.00 USD Received 9 Aug 2007; revised 18 Sep 2007; accepted 18 Sep 2007; published 25 Sep 2007

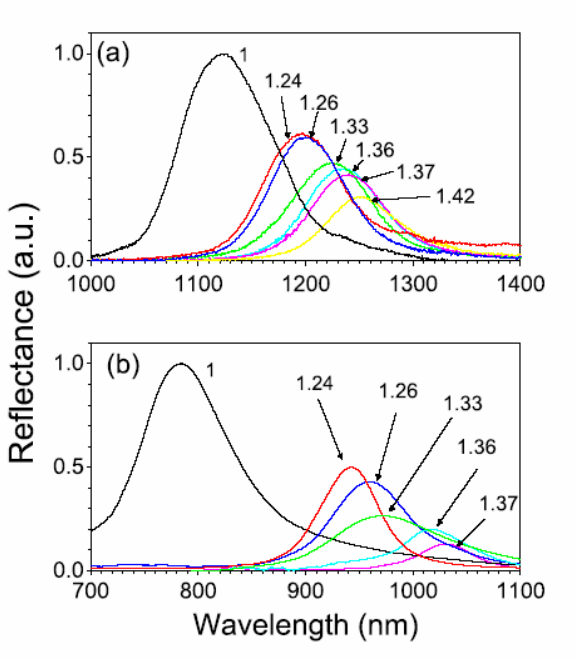

Fig. 4. Reflection spectra of direct (a) and inverse (b) opal structures with the same sphere diameter of 520 nm diameter in air (n = 1.0) and in liquid solutions having refractive index in the range from 1.24 to 1.42. The spectra were normalized to peak reflectivities of the respective samples in air.

In reality, both micro-spectroscopic setup and FTIR spectrometer with IR microscope attachment use focusing by objective lenses having NA = 0.75 and 0.5, respectively. Hence, incidence angles are distributed within the angular ranges of up to 50º and 32º with respect to the normal to (111) plane. In these circumstances full 3D photonic band structure of opal should be taken into account instead of the single direction in order to correctly determine the spectral positions of reflection peaks. In addition to the red shift, the reflection peaks become suppressed with increasing refractive index. This behavior is seen in Fig. 4, and is summarized in Fig. 6. The amplitudes of reflection peaks decrease nearly linearly with refractive index of the infiltrating material. One can extrapolate that the peaks will disappear completely at the refractive index values of ≈ 1.60 for direct and ≈ 1.46 for inverse opal, i.e., at vanishing index contrast.

3.3. Proposed utilization of inverse silica opal for optical sensing

To illustrate utilization of the spectral modifications described above for optical sensing, it is helpful to compare reflectivities of PhC structures infiltrated by materials with very close values of refractive index. As an example, in Fig. 7 we compare the pairs of spectra from Fig. 4 for inverse and direct opal PhCs infiltrated by solutions of FC72 (n = 1.24) and FC77 (n = 1.26). Despite the small index difference of $|\Delta n|$ = 0.02, the inverse structure [Fig. 7 (a)] generates strong differential reflectivity with symmetrical negative and positive wings having amplitudes of about 0.15. Notice, that these amplitudes constitute about 20-30% of the samples' reflectivity (≈ 0.5, see insets to Fig. 7) and hence can be easily detected in practice. One can expect that inverse opal will enable detection of index changes as small as 10^{-3}. In comparison, the direct opal structure [Fig. 7 (b)] has about twice lower sensitivity: its differential reflectivity has asymmetric shape with amplitude of the dominant negative wing of about 0.08. The lower overall sensitivity of direct opal can be expected, having in mind the dependencies shown in Fig. 4.

#86262 - $15.00 USD Received 9 Aug 2007; revised 18 Sep 2007; accepted 18 Sep 2007; published 25 Sep 2007

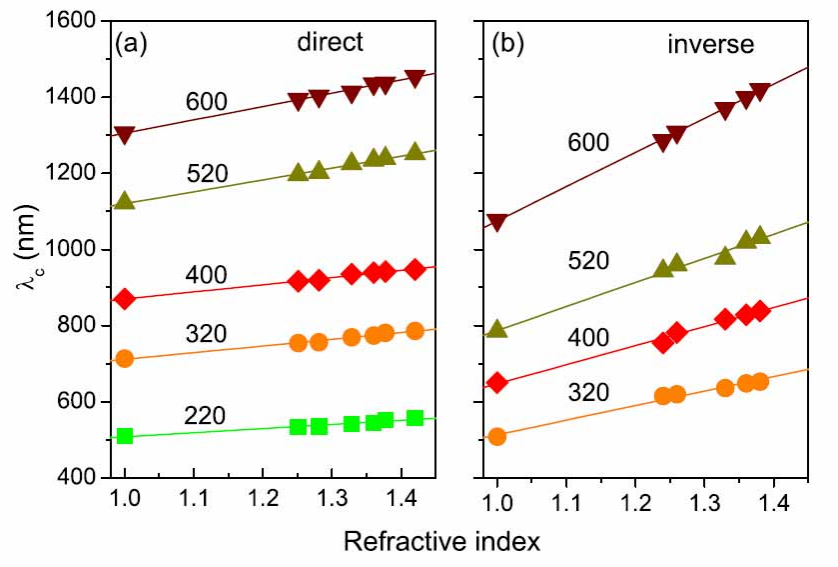

Fig. 5. Measured wavelength of PSG peaks versus refractive index of the environment in direct (a) and inverse (b) opal structures for different sphere diameters. The measured data are represented by symbols; the lines are linear fits to the experimental dependencies. Relative statistical variations of λ_c values are less than 1%.

It is helpful to notice that this kind of optical sensing can be realized by simple reflection (or transmission) measurements that register only the power flows of reflected and transmitted radiation. Transmission signal can be easily measured even in the near field, for example by sandwiching an inverse opal PhC film between a planar broadband source and a planar detector (with optional narrowband spectral filter). Hence, smaller sensors requiring simpler optical detection scheme would be achieved in comparison to sensors exploiting superprism effect [8].

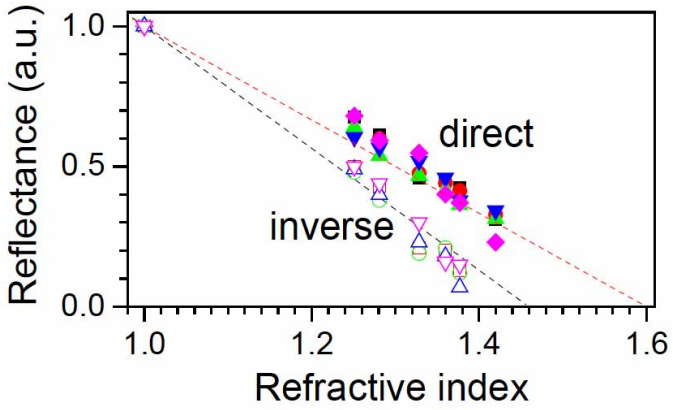

Fig. 6. Normalized magnitudes of reflection peaks versus the refractive index for direct and inverse opal structures. The particle diameters are: ♦ 220, ■ 320, ▲ 400, ▼ 520, and ● 600 nm.

#86262 - $15.00 USD Received 9 Aug 2007; revised 18 Sep 2007; accepted 18 Sep 2007; published 25 Sep 2007

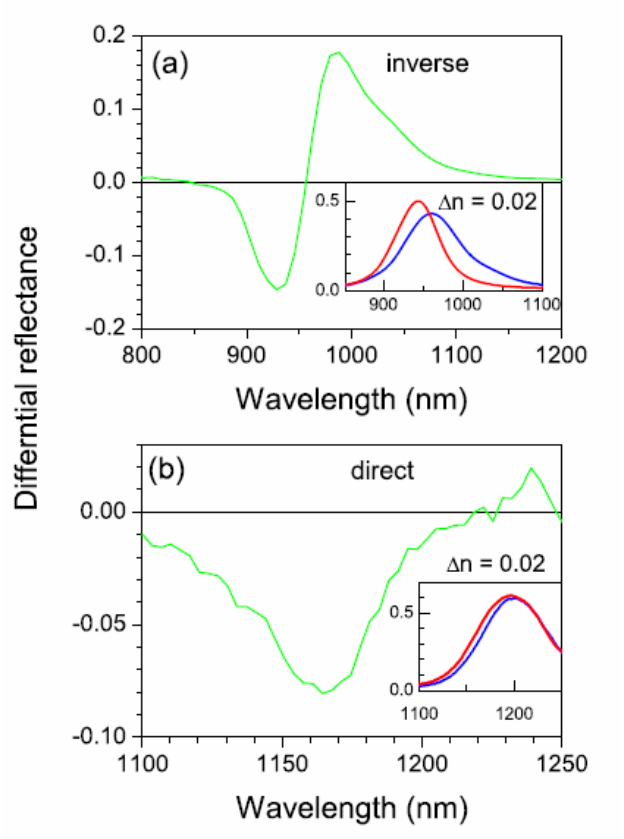

Fig. 7. Differential reflectance spectra for inverse (a) and direct (b) opal structures with sphere radius d = 520 nm, infiltrated by solutions of FC72 (n =1.24) and FC77 (n =1.26). In both panels the insets show the original reflectivities from Fig. 4.

4. Conclusions

Opal PhC structures from polystyrene microspheres of various sizes were prepared, and subsequently inverted using low-temperature silica sol-gel process. High quality of silica glass obtained using this process was confirmed. Comparison of optical properties of direct and inverse opal structures was conducted with aim to reveal potential benefits of inverse silica opal PhC structures for sensor applications. It was found that photonic stop gaps in inverse opals have about twice-higher sensitivity to the variations in the refractive index of environment, compared to direct opals. The inverse opal structure enables easy detection of index variations by $\Delta n = 0.02$ and has a tentative sensitivity limit of $\Delta n \sim 10^{-3}$, or of the same order of magnitude as that of optical sensors based on 2D photonic crystal microcavities [7] and photonic crystal fibers [9]. Although this result lags behind the $\sim 10^{-5}$ sensitivity inferred for opal sensors exploiting superprism effect [8] and colloidal tunable photonic crystals [22], these approaches require somewhat more complicated optical measurement schemes or sample preparation procedures. Silica inverse opal PhCs described in the present study does not require complicated fabrication procedures or optical measurement schemes, and yet can provide a substantial sensitivity. The simplicity of their preparation and application may be helpful for the integration of direct and inverse opal sensor elements into photonic or micro-fluidic chips [21]. Besides the improved sensitivity, the use of silica glass material allows application of PhC sensors in thermally and chemically harsh environments. These findings may help improve characteristics and widen the range of possible applications of optical sensors based on opal PhC structures.

#86262 - $15.00 USD Received 9 Aug 2007; revised 18 Sep 2007; accepted 18 Sep 2007; published 25 Sep 2007

Acknowledgments

H. M. is grateful for Grant-in-Aid from the Ministry of Education, Science, Sports, and Culture, Japan (No. 17360110) for partial financial support of the research.

#86262 - $15.00 USD Received 9 Aug 2007; revised 18 Sep 2007; accepted 18 Sep 2007; published 25 Sep 2007